In re: Mahajan et al..
Appl. No. 09/954,950
Filed September 18, 2001

APPENDIX TAB 5

Reduction of Stability of Arabidopsis Genomic and Transgenic DNA-Repeat Sequences (Microsatellites) by Inactivation of AtMSH2 Mismatch-Repair Function[1]

Jeffrey M. Leonard, Stephanie R. Bollmann, and John B. Hays*

Department of Environmental and Molecular Toxicology, Oregon State University, Corvallis, Oregon 97331-7301.

Highly conserved mismatch repair (MMR) systems promote genomic stability by correcting DNA replication errors, antagonizing homeologous recombination, and responding to various DNA lesions. Arabidopsis and other plants encode a suite of MMR protein orthologs, including MSH2, the constant component of various specialized eukaryotic mismatch recognition heterodimers. To study MMR roles in plant genomic stability, we used Arabidopsis *AtMSH2::TDNA* mutant SALK_002708 and *AtMSH2* RNA-interference (RNAi) lines. *AtMSH2::TDNA* and RNAi lines show normal growth, development, and fertility. To analyze *AtMSH2* effects on germ line DNA fidelity, we measured insertion-deletion mutation of dinucleotide-repeat sequences (microsatellite instability) at nine loci in 16 or more progeny of two to four different wild-type or AtMSH2-deficient plants. Scoring 992 total alleles revealed 23 (2.3%) unique and 51 (5.1%) total repeat length shifts ([+2], [−2], [+4], or [−4] bp). For the six longest repeat loci, the corresponding frequencies were 22/608 and 50/608. Two of four *AtMSH2-RNAi* plants showed similar microsatellite instability. In wild-type progeny, only one unique repeat length allele was found in 576 alleles tested. This endogenous microsatellite instability, shown for the first time in MMR-defective plants, is similar to that seen in MMR-defective yeast and mice, indicating that plants also use MMR to promote germ line fidelity. We used a frameshifted reporter transgene, $(C)_7$*GUS*, to measure insertion-deletion reversion as blue-staining β-glucuronidase-positive leaf spots. Reversion rates increased only 5-fold in *AtMSH2::TDNA* plants, considerably less than increases in MSH2-deficient yeast or mammalian cells for similar mononucleotide repeats. Thus, MMR-dependent error correction may be less stringent in differentiated leaf cells than in plant equivalents of germ line tissue.

Highly conserved protein systems are used by most organisms to preserve DNA integrity in the face of replication errors, attack from exogenous or endogenous mutagens, and spontaneous events such as deamination or depurination. Several challenges to genomic stability are unique to plant physiology and life forms. Unable to move, plants must cope with (sometimes obligate) exposure to environmental mutagens such as solar UV-B light or heavy metals. Oxygen-producing metabolism subjects cells to the mutational hazards of reactive oxygen species. Perhaps most important, plants lack a true reserved germ line; their gametes are derived from cells that have undergone many somatic divisions, with the potential for mutation fixation at each DNA replication. Although protective responses, such as production of UV-filtering flavonoids, may attenuate DNA damage, environmental challenges to the genome cannot be eliminated. Thus, plant genome maintenance systems at least as rigorous as those found in other organisms would seem essential. In fact, Arabidopsis orthologs of most gene products implicated in maintenance of genomic stability in other eukaryotes have been identified (for review, see Hays, 2002). We focus here on the multiprotein DNA mismatch repair (MMR) system.

Although DNA replicative polymerases copy template DNA with striking fidelity, incorrect bases are incorporated into nascent DNA at rates of 10^{-6} to 10^{-7} per base pair replicated. Insertions or deletions of nucleotides (potential frame shift mutations) may be more frequent where nucleotide-repeat sequences can give rise to slip-mispairing (for review, see Kunkel and Bebenek, 2000). The MMR system has evolved to correct a large portion of these errors, further reducing the error rate to 10^{-9} to 10^{-10}. Repair entails recognition of the mismatch, identification of the nascent strand for excision of DNA surrounding the mismatch, and DNA resynthesis, notably by a replicative polymerase, to fill the excision gap. The importance of such a system is evidenced by its high evolutionary conservation: All eukaryotes and most eubacteria examined have retained genes encoding homologous MMR proteins.

Mismatched bases also arise during recombination. MMR-mediated correction of occasional mismatched heteroduplexes formed during homologous recombination results in gene conversion. MMR also antagonizes homeologous recombination between di-

[1] This research was supported by the National Science Foundation (grant no. MCB 0078262 to J.B.H.) and by a National Institute of Environmental Health Science Training Grant (grant no. 1P42 ES10338 to S.R.B.).

* Corresponding author; e-mail hays@bcc.orst.edu; fax 541–737–0497.

Article, publication date, and citation information can be found at www.plantphysiol.org/cgi/doi/10.1104/pp.103.023952.

verged but similar sequences, apparently in response to mismatches in recombinational intermediates (Chambers et al., 1996). Within a species, this may prevent chromosomal rearrangement, by aborting recombination between duplicated genes. Antagonism of recombination between dissimilar sequences also presents a genetic barrier to interspecies crosses (Matic et al., 1995). The recent demonstration (Dong et al., 2002) that a wheat (*Triticum aestivum*) MMR homolog (*MSH7*; see below) is linked to a mutation (*ph2a*) known to increase recombination frequency in wide crosses is interestingly consistent with this observation, although direct involvement of the gene product has yet to be proven.

Seven homologs of the prototypic prokaryotic MutS protein (MSH) have been identified in eukaryotes, at least three of which (MSH2, MSH3, and MSH6) have been firmly implicated in mismatch correction (for review, see Kolodner and Marsischky, 1999). Mismatch recognition, the responsibility of MutS homodimers in bacteria, is accomplished by MutSα (MSH2·MSH6 heterodimer) in the case of base-base mispairs or single extrahelical nucleotides, or by MutSβ (MSH2·MSH3 heterodimer) for larger extrahelical loopouts. Similarly, the bacterial MutL homodimer, thought to couple mismatch recognition to identification and excision of the nascent strand, is replaced by MutL-homolog (MLH1·PMS2) heterodimers for most post-replication error correction. *Escherichia coli* and some other bacteria identify nascent strands by their transitory non-methylated d(GATC) sites, which their MutH proteins nick when stimulated by mismatch-bound MutS and MutL. Many bacteria and all eukaryotes lack GATC methylation and MutH homologs; by one hypothesis, they use instead the 3′ ends of nascent DNA or 5′ ends of Okazaki fragments as a basis for strand identification.

A seventh MSH has been identified in Arabidopsis (Culligan and Hays, 2000) and other plants (Horwath et al., 2002) but not thus far in animals. AtMSH7 is most similar to AtMSH6 and also forms heterodimers in vitro with AtMSH2 (designated MutSγ), but the heterodimers exhibit somewhat different affinities for the range of mismatches. AtMSH2-AtMSH6 and AtMSH2-AtMSH7 heterodimers may perform overlapping as well as unique roles in base-mismatch recognition in plants (Culligan and Hays, 2000). Despite the apparent need for rigorous genome maintenance and the presence of clear orthologs of MMR proteins, a recent study found somewhat higher somatic mutation rates in leaves than have been observed in other organisms (Kovalchuk et al., 2000). This puts into question the role of MMR in planta.

Microsatellites, simple repeats of one or a few nucleotides, are found throughout eukaryotic genomes. Microsatellite instability, manifested as repeat length polymorphisms, is a hallmark of MMR deficiency and is used clinically to assess MMR proficiency in mammalian tumors. Instability is thought to arise during replication, when transient melting and out-of-frame re-annealing of nascent and template DNA strands in repeat regions cause extrahelical loopouts that escape proofreading by replicative polymerases. These are corrected efficiently by MMR in wild-type cells, but in MMR-deficient cells, rates of insertion-deletion mutations, especially at longer repeat sequences, increase dramatically—as much as 4 orders of magnitude in long mononucleotide runs (Tran et al., 1997).

To investigate the role of MMR in plant genomic stability, we analyzed effects of deficiency in the essential MMR protein AtMSH2, the constant component in MutSα, MutSβ, and MutSγ. Insertion-deletion mutations in endogenous repeat sequences in a minority of the cells of an organism are difficult to detect in a background of normal sequences. We have circumvented this problem in two ways. First, we constructed frame-shift reporter transgenes by inserting out-of-frame repeat sequences in the *uidA* (*GUS*) gene and scoring revertant cells as blue spots—positive staining for β-glucuronidase (GUS)—in transgenic AtMSH2-deficient and -proficient plants. Second, the sequences at several endogenous microsatellite loci of multiple progeny from AtMSH2-defective plants, some of which might be expected to be homozygous or heterozygous for insertion-deletion mutations that occurred in the parent, were compared with microsatellite sequences in progeny of wild-type plants. We used these assays to demonstrate microsatellite instability in plants in which *AtMSH2* was disrupted by a T-DNA insertion or a transgene that caused RNA interference (RNAi) of *AtMSH2* expression. The effect of MSH2 deficiency on generation and transmission of altered repeat length alleles appears similar to that seen in other higher eukaryotes, clearly implicating MMR in maintaining plant genomic stability. However, the MMR-deficient phenotype scored in leaf tissues appears less pronounced.

RESULTS

Identification of an *AtMSH2::TDNA* Plant

We identified two putative *AtMSH2* insertion-mutations, SALK_002707 and SALK_002708, in the Salk Institute T-DNA insertion library database (http://signal.salk.edu/cgi-bin/tdnaexpress) by a BLAST search. PCR screening of plants from each line with pairs of primers respectively specific for *AtMSH2* or T-DNA revealed in SALK_002708 a T-DNA insertion beginning in *AtMSH2* exon 7. The DNA sequence of the PCR products showed the T-DNA left border beginning after bp 2,714, the T-DNA right border region followed by the final 37 bp of the coding region, and deletion of 1,510 bp of *AtMSH2* between the two junctions (Fig. 1). Besides interrupting the coding sequences, the T-DNA insertion caused deletion of two highly conserved MSH2

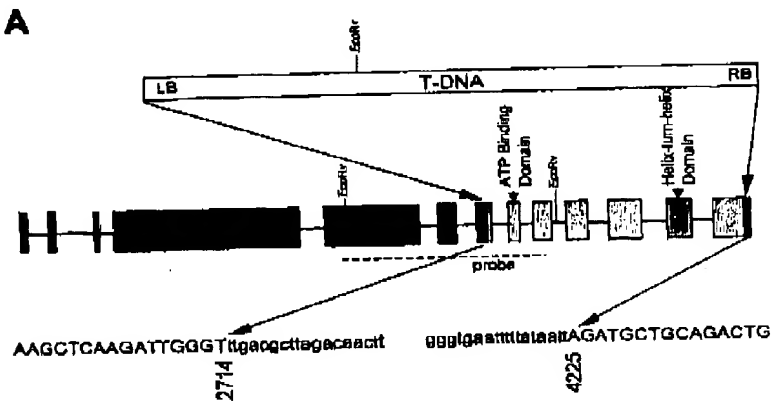

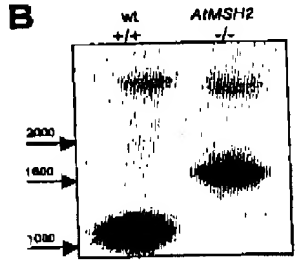

Figure 1. Structure of T-DNA insertion in *AtMSH2*. A, Sequences of PCR products generated with gene-specific and T-DNA-specific primers were used to deduce the structure of the disrupted *AtMSH2* in the line SALK_002708. A single insertion of pROK2 T-DNA at positions 2,714 and 4,225 caused deletion of exons 8 to 12 and portions of exons 7 and 13 (gray boxes) in this line. Sequences of junction regions are below. Capital letters indicate *AtMSH2* and lowercase letters indicate the insertion, beginning 2 bp downstream of the left border at the exon 7 junction and preceded by approximately 150 bp of rearranged sequence following the right border at the exon 13 junction. B, DNA blot of *Eco*RV-digested wild-type and T-DNA insertion homozygotes probed with a radiolabeled *AtMSH2* fragment (dashed line).

regions essential for function, the ATP-binding domain and the helix-turn-helix domain (Alani et al., 1997).

Progeny of all eight T_3 generation SALK_002708 plants tested were found to be homozygous for the T-DNA insertion. DNA-blot (Southern) analysis confirmed the presence of the predicted 1.8-kb *AtMSH2*::*TDNA* fragment (Fig. 1). No morphological abnormalities of *AtMSH2*::*TDNA* plants were apparent, and seed sets and germination rates were not significantly different from those of wild-type plants (data not shown).

Analysis of Repeat-Sequence Insertion-Deletion Mutation with Frame-Shifted GUS Transgenes

To quantitatively analyze insertion-deletion mutations of specific repeat sequences (microsatellites)—ultimately in a variety of genetic backgrounds—we constructed a series of *GUS* transgene alleles containing out-of-frame mono- or dinucleotide repeats and introduced them into Arabidopsis. A similar approach was used by Kovalchuk et al. (2000), who measured base-substitution reversion of nonsense codons in a series of GUS-transgene alleles by histochemical detection of *GUS*$^+$-revertant (blue) spots in whole plants. Previously, a number of investigators had observed highly elevated rates of frame-shift reversion of reporter alleles in MMR-deficient *E. coli* (Cupples et al., 1990), yeast (Strand et al., 1993), and mammalian cells (Parsons et al., 1993), consistent with instability of endogenous microsatellite sequences in MMR-deficient human tumors (Loeb, 1994).

We inserted frameshifting $(G)_7$, $(G)_{10}$, $(G)_{13}$, or $(AC)_{17}$ runs near the 5′ end of the GUS coding sequence. When a *GUS* control allele (containing an in-frame $(G)_{12}$ run), was transformed into Arabidopsis, 35 of 36 lines (progeny of independent transformation events) stained completely blue, demonstrating that the amino acids encoded by the repeated nucleotides did not significantly decrease GUS activity. To eliminate ambiguities that might be caused by T-DNA (GUS) insertions at multiple loci, we identified transformed lines whose T_2 progeny segregated 3:1 for antibiotic resistance. Plants from these putative single-locus lines harvested after 2 weeks, then stained with 5-bromo-4-chloro-3-indolyl-β-D-glucuronide for detection of GUS activity and decolorized, were generally white; GUS activity was seen primarily in spots varying from single cells to 1 mm in diameter, and more rarely seen in sectors.

Initially, approximately 35 plants—corresponding to a total of roughly 2.4×10^6 cell divisions (see "Materials and Methods")—of each of the independent single-locus transformed lines were analyzed for each *GUS* allele. GUS activity was detected by staining in plants from all six $(G)_{13}GUS$ lines, but no GUS activity was detected in five of 11 $(G)_7GUS$ lines, one of six $(G)_{10}GUS$ lines, or one of 17 $(AC)_{17}GUS$ lines. We did not determine whether GUS-negative lines contained inactive copies of *GUS* or transgenes whose location caused expression or reversion levels to be below the limit of detection. The frequency of spots varied more than 10-fold among independent lines transformed with $(G)_7GUS$ or $(G)_{10}GUS$, and varied more than 2 orders of magnitude among independent lines carrying $(G)_{13}GUS$ or $(AC)_{17}GUS$. Kovalchuk et al. (2000) similarly observed a wide range of base-substitution reversion rates for the same allele in independent transformants. Nonetheless, there was a trend of increasing spot frequency with repeat length; the average numbers of spots/plant for all plants carrying the same allele were 0.6, 1.2, 11.2, and 30.5 for $(G)_7GUS$, $(G)_{10}GUS$, $(G)_{13}GUS$, and $(AC)_{17}GUS$ lines, respectively.

We used Southern blotting of single-locus *GUS*-transformed lines to identify single-locus single-copy lines for further study. To confirm our assumption that increased mutation rates would be detectable by an increase in the frequency of GUS^+ spots, we subjected two different single-copy $(G)_7GUS$ lines to UV-C light (1,200 J m^{-2}), a mutagen shown to increase frameshifts at repeat sequences in bacteria (Cupples et al., 1990). In each line, UV-C light increased GUS^+ spot frequencies approximately 5-fold (data not shown). For comparison, strong doses of UV-C light stimulated (+1) and (−1) frameshift reversions at $(G)_6$ runs in the *lac*Z gene by factors of five to 20 (Cupples et al., 1990). Thus the observed GUS^+ spots most likely correspond to (−1) deletions and (+2) insertions at the $(G)_7$ runs.

We chose a single-copy $(G)_7GUS$ line ($(G)_7$GUS-1) selfed to homozygosity for further studies for two reasons. First, the typical reversion frequency of this line—one spot per plant—was high enough to generate statistically significant data using a reasonable number of plants, but could be accurately scored. In contrast, the typically high spot numbers in plants with longer-repeat alleles (more than 50 per plant in six of 17 $(AC)_{17}$ *GUS* lines) made quantitative scoring problematic. Second, line $(G)_7$GUS-1 exhibited a stable mutation rate, approximately 0.9 spots per plant, in three successive generations (Table I).

Reversion Mutation of Transgene Repeat Sequences in AtMSH2-Defective Plants

In comparing *GUS* reversion rates, we wanted to minimize any background variations, such as in *GUS* expression, that might arise during propagation of MMR-deficient and -proficient lines. Therefore we chose to analyze segregating F_2 progeny of single F_1 parents heterozygous or hemizygous for *AtMSH2::TDNA* and for (single-copy) $(G)_7GUS$-1 alleles, respectively. First, we crossed Arabidopsis line $(G)_7$GUS-1 with an $AtMSH2^{-/-}$ plant. A resultant F_1 plant was selfed, yielding F_2 progeny whose *AtMSH2* genotypes were determined by diagnostic PCR of DNA extracted from single cotyledons excised before GUS staining. The $(G)_7GUS$-1 genotype was similarly confirmed by diagnostic PCR with *GUS*-specific primers, and only those progeny shown to carry the $(G)_7GUS$-1 allele were scored for blue spots. Both $AtMSH2^{+/+}$ and $AtMSH2^{+/-}$ F_2 progeny showed approximately one spot per plant, similar to the rate for the original $(G)_7$GUS-1 parental line (Table I). However, F_2 $AtMSH2^{-/-}$ progeny exhibited approximately five times as many blue spots per plant. To confirm these results, some of the F_2 plants homozygous for both the $(G)_7GUS$-1 allele and either $AtMSH2^{+/+}$ or $AtMSH2^{-/-}$ were selfed to produce F_3 progeny. The rate of reversion in F_3 $(G)_7GUS$-1/$AtMSH2^{+/+}$ plants was similar to the original parental $G_{(7)}$GUS-1 line (Table I), indicating that segregating the T-DNA insertion away had restored wild-type function of *AtMSH2*. However, F_3 $(G)_7GUS$-1/$AtMSH2^{-/-}$ progeny reverted at approximately 5-fold the wild-type rate, similar to $AtMSH2^{-/-}$ F_2 progeny.

Table I. *Insertion-deletion reversion of $(G)_7GUS$ transgenes*

Generations after Transformation with $(G)_7GUS$	Genotype (n)[a]	GUS^+ Revertant Spots per Plant[b]
T_2	*AtMSH2* +/+ (103)	1.0 (±0.3)
T_3	*AtMSH2* +/+ (87)	1.2 (±0.2)
T_4	*AtMSH2* +/+ (98)	0.9 (±0.2)
T_5[c]	*AtMSH2* +/+ (9)	1.2 (±1.0)
	AtMSH2 +/− (27)	0.9 (±0.6)
	AtMSH2 −/− (17)	5.7 (±0.8)
T_6[d]	*AtMSH2* +/+ (92)	0.8 (±0.2)
	AtMSH2 −/− (114)	5.2 (±0.9)

[a] Number of plants analyzed. [b] Means (95% CI) for 2-week-old plants. [c] F_2 progeny segregating for *AtMSH2::TDNA*. [d] F_3 progeny homozygous for wild-type or mutant *AtMSH2* allele.

Instability of Endogenous Microsatellite Sequences in MMR-Defective Plants

We considered it essential to analyze effects of plant MMR deficiency on endogenous repeat sequences for several reasons. Microsatellite instability in a variety of MMR-deficient mammalian cells and whole animals has been extensively studied, providing a basis for comparisons with observations in plants. Because a large number of Arabidopsis and other plant microsatellite sequences have been identified, it was possible to choose a variety of repeat units and repeat lengths, whereas only the $(G)_7$*GUS* allele was convenient for extensive studies. Furthermore, because detection of expansions/contractions of microsatellite sequences does not depend on gene expression, one potential source of variation among sublines—epigenetic effects on gene transcription, which might affect detectability of *GUS*$^+$ revertant and/or transcription-coupled repair of endogenous DNA damage—was eliminated, although chromosomal location might affect mutation rates by other mechanisms. Finally, the appearance (or not) of microsatellite length polymorphisms in the (multiple) progeny of a single parent would reflect events in the equivalent of a plant germ line: the floral tissues, the meristematic tissues that give rise to them, and the ancestry of the latter. In contrast, the total of *GUS*$^+$ revertant (frameshifted) spots scored in whole plants is dominated by events in differentiated leaf cells, which might be subject to less rigorous genomic stability maintenance than the quasi-germ line cells.

We chose for analysis high multiple repeats of dinucleotide units—to increase the likelihood of slippage and to enhance resolution respectively—that were scattered throughout the genome. Of 10 such microsatellite loci originally identified, nine could be efficiently PCR-amplified using primers that yielded 154- to 318-bp products, most of which could be resolved by capillary electrophoresis. By choosing primers labeled with different fluorescent dyes where product sizes were close, we were able to analyze mutations (if any) at nine different loci (18 alleles) in each electropheresis run (Fig. 2A). The electropherograms of PCR products templated with individual progeny DNA clearly indicated shifts in repeat lengths (insertions or deletions) of one or more 2-bp units at either one or both alleles at each locus (Fig. 2B). By mixing DNA from two plants, each known to be homozygous for a different repeat length at a particular locus, we reconstructed these patterns and confirmed our ability to deduce genotypes from electropherograms (Fig. 2C). When mixed at a ratio of≥4:1, the minority DNA product was undetectable, strengthening our conclusion that alleles measured in progeny originated in the parent and were transmitted through the germ line. Novel alleles that arose after the 8- or 16-cell stage of progeny development would represent much less than

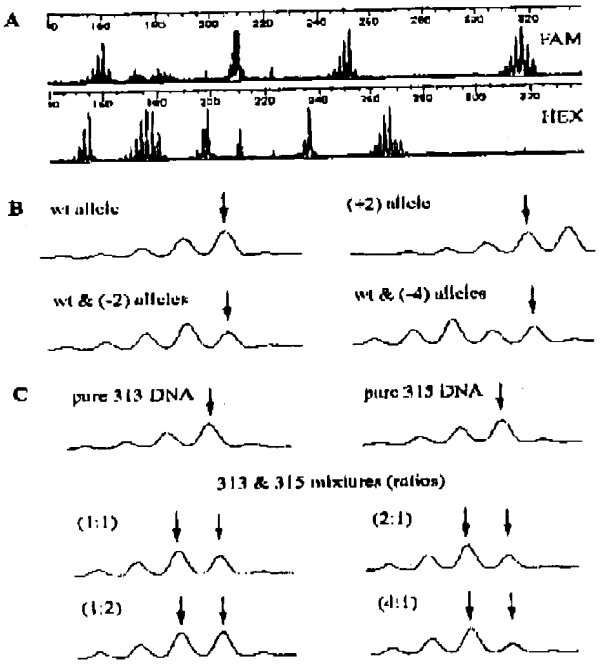

Figure 2. PCR amplification of DNA containing each of nine different microsatellites from each progeny plant with one of each locus-specific primer pairs, analysis of product mixtures by capillary electrophoresis, detection of fluorescent products, and generation of electropherograms were as described under "Materials and Methods." A, Electropherograms showing all PCR products; one of each primer pair was labeled with FAM or HEX fluorescent dye. B, Representative electropherogram patterns for locus NGA1107. Apparent absolute size of primary wild-type (wt) product band is 317 bp. Shown also are products where both alleles showed an increase of one repeat unit, increasing apparent product length to 319 bp (+2), where one allele maintained wild-type length and one showed a loss of one repeat [wt & (−2)], and where one allele remained wild type and one showed a shift of two repeats, decreasing apparent length to 313 bp [wt & (−4)]. Arrows indicate position of 317-bp (wild-type) product. C, Patterns for reconstruction mixtures. DNA from plants homozygous (pure) for alleles at locus NGA1107 encoding 313-bp (black arrow) or 315-bp (gray arrow) products or mixtures of the two at indicated ratios (concentrations of DNAs measured before PCR by staining with PicoGreen [Molecular Probes, Eugene, OR]) were analyzed as described above. Note that the primary criterion for scoring a pattern as reflecting a mixture of two different length products—second peak from right greater than a significantly large first peak—is met only for 1:1 and 2:1 mixtures.

20% (4:1 mix) of total alleles present and would thus be undetectable in our measurements.

Table II shows analyses of progeny of two wild-type and three *AtMSH2*$^{-/-}$ plants: a total of 576 alleles from *AtMSH2*$^{+/+}$ plants and 992 alleles from *AtMSH2*$^{-/-}$ plants. We detected only one unique repeat length change (both altered in one plant) in

Table 11. *Effects of AtMSH2 disruption on stability of nucleotide-repeat sequence (microsatellite) alleles*

Frequencies of unique and total repeat-length shifts at indicated loci in progeny of indicated plants.

	AtMSH2::TDNA$^{-/-}$			*AtMSH2*$^{+/+}$	
Locus[a]	1[c]	2[d]	3[e]	1[c]	2[d]
AtEAT	1.6[n] (1.6)	0	0	0	0
$(AT)_{11}$ TJFI7	0	0	0	0	0
$(AG)_{15}$ NGA16B	0	0	0	0	0
$(CT)_{20}$ NGA8	3.1[q/r](7.8)	3.1[f] (9.4)	3.1[n] (9.4)	0	0
$(AG)_{35}$ NGA172	1.6[f] (1.6)	6.2[n/r](9.4)	3.1[f] (3.1)	0	0
$(TC)_{26}$ NGA107	hel[h]	6.2[q/r](12.5)	3.1[n] (9.4)	0	0
$(CT)_{27}$ NGA151	3.1[n/r](14.1)	hel[h]	6.2[n/r](9.4)	0	0
$(TG)_{29}$ NGA6	hel[h]	6.2[n/r](6.2)	3.1[n] (9.4)	0	0
$(AG)_{11}$ NGA139	3.1[q/r](7.8)	3.1[f] (6.2)	3.1[n] (9.4)	3.0[q/r](7.1)	0
$(TC)_{11}$					

[a] Thirty-two progeny (64 alleles per locus) examined. [b] Sixteen progeny (32 alleles per locus) examined. [c] Fourteen progeny (28 alleles per locus) examined. [d] Eighteen progeny (36 alleles per locus) examined. [e] (+2) shift. [f] (−2) shift. [g] (+4) shift. [h] Parent already heterozygous at this locus. [i] (−4) shift.

the wild-type plants, but we detected 23 unique length changes and a total of 51 length changes in the *AtMSH2* $^{-/-}$ progeny. As expected, most shifts occurred in higher repeat length loci: only once among all three loci of 20 repeat units or less, but at least once in all loci with 25 or more repeats. Where a single shift, e.g. (+2), is seen in multiple progeny from the same parent, we cannot distinguish among a single shift early in the lineage of a parental plant that gave rise to a clone of parental cells with the same new allele, multiple independent events that produced that allele, or an intermediate situation. In all cases, several progeny might show the same shift. Thus, Table 11 shows both the frequency of unique repeat length shifts observed among all targets tested for each locus (typically two alleles for each of 16 plants), expected to be at most 9.4% or 12.6% (three or four unique shifts in 32 targets), and total length shifts observed, which could in principle be 100%, if parental lengths in both alleles were altered very early in development and all progeny were derived from cells with altered-length alleles. Figure 3 shows that for all loci in *AtMSH2::TDNA* plants, the mean frequency of unique repeat length shifts per allele was 2.3%, compared with 0.2% for the single repeat length shift in *AtMSH2*$^{+}$ plants. When we considered the subset of loci with 25 or more repeat lengths, the frequencies were 3.6% versus 0.3%. In the case of two loci, NGA6 and NGA1107, the different lengths observed in the progeny of *AtMSH2*$^{-/-}$1 (Table II) were present at predicted Mendelian ratios for an already-heterozygous parent, as if in each case, a (+2) length shift had occurred at both loci early in the development of the parent plant or had occurred in its parent. A similar result was observed at locus NGA151 in the progeny of *AtMSH2*$^{-/-}$2 (Table II). These preexisting shifts were not included in the tabulated data, but no such patterns were observed in the *AtMSH2* $^{+}$ plants, where MMR is expected to correct microsatellite slippage.

Inactivation of AtMSH2 by RNAi

We also inactivated MMR via double-stranded RNAi. A fragment of *AtMSH2* DNA was ligated in sense and antisense orientations on opposite sides of an 1.4-kb stuffer (intron) fragment, creating binary vector pMSH2(RNAi). This was transformed into Arabidopsis in parallel with transformation with vector-only (pPGC5941) controls. T_2 progeny carrying at least one copy of the transgene were analyzed for insertions/deletions at the same endogenous microsatellite loci as described above.

Line-to-line phenotypic variability is well documented in RNAi-mediated suppression in plants (Chuang and Meyerowitz, 2000), so we expected to detect microsatellite alterations more frequently in some RNAi-transformed lines than in others. Progeny of four lines (independent transformations) were analyzed for endogenous microsatellite instability by the PCR-electrophoresis technique (Table III). One line, MSH2(RNAi-3), showed no repeat length shifts in the 288 alleles assayed. However, length shifts were detected in the remaining three lines at varying frequencies. In 16 progeny of MSH2(RNAi-1), MSH2(RNAi-2), and MSH2(RNAi-4), there were eight, four, and three unique length shifts, respectively, equivalent to frequencies of 2.8%, 1.4%, and

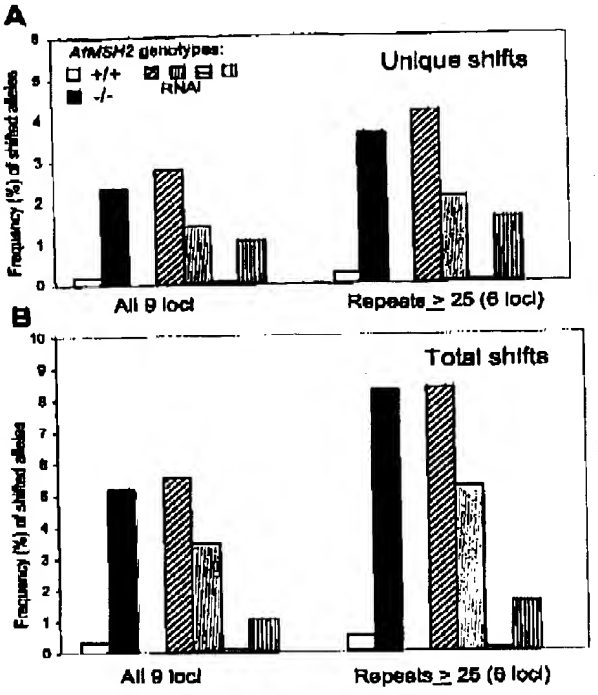

Figure 3. Frequency (%) of repeat length-shifted alleles in endogenous microsatellite loci. Frequencies were calculated by dividing numbers of unique length shifts (A) or total numbers of all alleles showing non-parental lengths (B) in the progeny of two *AtMSH2*$^{+/+}$ plants or of three *AtMSH2*$^{-/-}$ plants or of four individual *AtMSH2(RNAi)* plants by the total number of alleles tested in each group. Data represent sums for all nine loci analyzed or for the six loci with ≥25 repeat units. No length shifts were detected in progeny of two plants transformed with the empty binary vector pPGC5941.

1.0%. The frequencies of unique shifts in progeny of lines MSH2(RNAi-1) and MSH2(RNAi-2) approached those observed in *AtMSH2*$^{-/-}$ insertion-mutant plants (Table III; Fig. 3). As in earlier measurements, mutations were more frequent at loci with ≥25 repeat units. For repeat lengths ≥25 units, the frequencies of unique and total length-shifted alleles for the two high RNAi lines were 3.1% and 6.8%, respectively, similar to those for *AtMSH2*$^{-/-}$ plants—no length shifts occurred in loci with repeats less than 20 in length.

To ensure that the observed length shifts were the result of RNAi interference and were not an artifact of T-DNA transformation, we analyzed shifts in two lines transformed with empty vectors. The progeny of one plant segregated for two alleles at locus NGA 151, indicating that the parent was heterozygous; as in the case of *AtMSH2::TDNA* plants heterozygous for two microsatellite alleles (see above), these data were not included in our calculations. No other shifts were detected in any of the 544 other alleles assayed, indicating that the observed shifts in the RNAi lines were due to interference with *AtMSH2* mRNA stability by the product of the dsRNA-producing vector pMSH2(RNAi).

DISCUSSION

Arabidopsis and other higher plants whose genomes have been analyzed thus far encode suites of MSH and MLH proteins highly similar to other eukaryotic MMR proteins, plus an extra mismatch recognition component apparently unique to plants, MSH7 (Hays, 2002). Initial biochemical studies of mismatch recognition by MSH2·MSH3, MSH2·MSH6, and MSH2·MSH7 heterodimers (Culligan and Hays, 2000) suggest but do not prove that MSH/MLH systems correct DNA replication errors and antagonize homeologous recombination in plants, as in other organisms. Here, we have analyzed the effects of inactivation in Arabidopsis of *AtMSH2*—the constant component of all mismatch recognition complexes—by gene disruption or RNAi. The dramatic increases in insertion-deletion mutation of endogenous nucleotide repeat sequences (microsatellite instability) measured in the progeny of AtMSH2-deficient plants are similar to those seen in MMR-defective mammalian and yeast cells, for the first time directly implicating plant MSH proteins—and by extension MLH proteins—in maintenance of plant genomic stability. *AtMSH2* disruption also increases insertion-deletion mutation of synthetic repeat sequences in GUS reporter transgenes, mostly in leaves, but to a considerably lesser extent than increases seen for similar repeat sequences in yeast and mammalian cells.

AtMSH2::TDNA homozygotes were recovered in Mendelian ratios from segregating populations and exhibited wild-type seed sets and germination rates. This apparent absence of reduced fitness is consistent with the normal viability of MSH2-deficient mice (Reitmair et al., 1995) and yeast (Reenan and Kolodner, 1992). Nonetheless, it would seem that if MMR functions in plants as it does in other organisms, these and other MMR-defective plants would accumulate errors detrimental to overall fitness over the course of generations. Such a cumulative decrease in fitness has recently been described in MMR-defective *Caenorhabditis elegans* (Degtyareva et al., 2002), and we are carrying out similar long-term studies.

Instability of microsatellite sequences—that is, expansion/contraction of long repeats of one to four nucleotides—has long been a hallmark of MMR deficiency, particularly in mammalian cells. In the absence of a reserved plant germ line, the nearest thing to a measure of germ line mutation rates would seem to be frequencies of microsatellite length shifts among the progeny of a single parental plant, reflecting events not only during floral development, but

Table III. *Effects of AtMSH2 RNA-interference on stability of nucleotide-repeat sequence (microsatellites) alleles*

Frequencies of unique and (total) repeat-length shifts at indicated loci in progeny of indicated plants.

Locus	*AtMSH2(RNAi)*				Empty Vector[a]	
	1[b]	2[b]	3[b]	4[b]	1[b]	2[b]
AtEAT	0	0	0	0	0	0
$(AT)_{11}$ T3F17	0	0	0	0	0	0
$(AG)_{15}$ NGA168	0	0	0	0	0	0
$(CT)_{20}$ NGA8	0	0	0	0	0	0
$(AG)_{25}$ NGA172	0	6.2[c,d] (25.0)	0	0	0	0
$(TC)_{26}$ NGA1107	9.4[c,d,e] (25.0)	3.1[d] (3.1)	0	6.2[e,f] (6.2)	0	0
$(CT)_{27}$ NGA151	0	0	0	3.1[e] (3.1)	het[g]	0
$(TC)_{29}$ NGA6	9.4[c,d,e] (9.4)	0	0	0	0	0
$(AG)_{31}$ NGA139	6.2[c,d] (15.6)	3.1[d] (3.1)	0	0	0	0
$(TC)_{33}$						

[a] Transformed with empty vector pFGC5941. [b] Sixteen progeny (32 alleles per locus) examined. [c] (+2) shift. [d] (−2) shift. [e] (+4) shift. [f] (+4) shift. [g] Parent already heterozygous at this locus.

also during division of meristematic cells in the lineage of floral precursors. We cannot distinguish between specific single parental microsatellite repeat length shifts that give rise to multiple shifted progeny and multiple independent parental shifts of the same type, so the minimum estimate of instability would be the number of unique shifts—(+2), (−2), etc.—among the total alleles (progeny × loci×2) tested: 2.3% for all loci and 3.6% for all repeats of 25 units or more for *AtMSH2::TDNA* plants; 0.2% and 0.3%, respectively, for AtMSH2$^+$ plants. For the six loci with repeat lengths of 25 or greater (NGA6, NGA8, NGA139, NGA151, NGA172, and NGA1107), the progeny of all three *AtMSH2::TDNA* plants analyzed showed at least one shift at every locus, except for the two cases—progeny of plant 2 at locus NGA151 and progeny of plant 1 at loci NGA6 and NGA1107—where parental plants were already heterozygous, indicative of shifts earlier in their ancestry; analysis was impossible in these cases. In comparison, 11.5% of 771 dinucleotide-repeat alleles analyzed in sperm from MMR-defective male mice showed repeat length shifts (Baker et al., 1995), and 74 of 816 (9.5%) of maternal alleles analyzed in (MMR-proficient) progeny of a MMR-deficient female crossed with a wild-type male mouse showed length shifts (Gurtu et al., 2002). These frequencies for MMR-defective mice again reflect both unique events and single length shift events yielding multiple progeny, and so appear similar to the 5.1% (all loci) and 8.2% (≥25 repeat loci) frequencies that we observed for MMR-defective plants. In addition, Gurtu et al. (2002) observed two shifts in 816 paternal alleles analyzed from progeny of a wild-type male and a MMR-deficient female, similar to the one unique (two total) repeat length shift(s) at locus NGA139 that we observed in 578 alleles analyzed in progeny from wild-type parents. Thus MMR deficiency appears to have similar effects on germ line genomic stability in plants and mammals.

Previous measurements of *AtMSH2*, *AtMSH3*, and *AtMSH7* mRNA levels (Ade et al., 1999) have suggested that expression of MMR genes is quite low in leaves (and perhaps other differentiated tissues), perhaps because DNA replication fidelity is not critical during the last few cell divisions in these tissues or during the DNA endoreduplication that follows (Galbraith et al., 1991). Because *GUS* mutation-reversion events were mostly scored as blue-staining spots in leaves, apparent spontaneous mutation rates might therefore appear higher than those observed in other systems—mammalian cells dividing in culture for example. Kovalchuk et al. (2000) reported rates of base-substitution reversion of 10^{-7} to 10^{-8} per generation in wild-type plants, 2 orders of magnitude higher than rates estimated for other organisms, although the large differences in rates for the same alleles in independent sub-lines made it difficult to determine true basal rates. If in fact MMR control of genomic fidelity is relaxed in leaves, then nucleotide-repeat sequences (microsatellites), whose insertion-deletion rates typically show dramatic increases in MMR-defective cells, would provide a sensitive test. For example, Tran et al. (1997) reported increases of more than 6,000- and 400-fold in mutation of $(A)_{10}$ and $(A)_7$ runs respectively in MMR-deficient yeast. An $(A)_{14}$ run mutates at a rate of 1.6×10^{-7} in wild-type yeast cultures, as estimated by standard fluctuation test techniques (Tran et al., 1997). In

2-week-old $(G)_{13}$*GUS*-Arabidopsis plants containing approximately 6.7×10^6 cells (see "Materials and Methods"), we measured an average of 11.2 GUS^+ spots per wild-type plant, a mutation rate of 2×10^{-6} per division. Although our G runs might mutate slightly more rapidly than the yeast A runs (Boyer et al., 2002), the apparent plant (leaf) insertion-deletion mutation rate was thus an order of magnitude higher than in yeast. Similarly, the basal rate of reversion of $(G)_7$*GUS* transgenes, about one per plant (2×10^{-7}), was 2 orders of magnitude greater than the rate of reversion of an $(A)_7$ run in yeast. Thus the relatively small increase in reversion of $(G)_7$*GUS* in *AtMSH2*$^{-/-}$ plants—only 5-fold versus 100-fold for $(A)_7$ runs in yeast—may reflect the lack of efficient MMR in differentiated tissues, so that reversion rates are already high even in the leaves of MMR-proficient plants.

Our studies thus indicate that by the criterion of parent-to-progeny microsatellite stability, plant germ line cells use MMR to correct primer-template slipmispairs—and by extension other premutational substrates—as efficiently as do yeast and mammals. However, in leaf and perhaps other plant differentiated cells, differences between MMR-deficient and -proficient plants are not as dramatic as in yeast or mammalian cells. In mammalian somatic cells, mutations that give rise to tumorigenesis pose a threat to survival of the organism, so the considerable energy cost of MMR—synthesis of multiple large proteins and replacement of hundreds of nucleotides per correction event—would seem justified, but this may not be the case in plant somatic cells.

MATERIALS AND METHODS

Growth of Plants

All plants were ecotype Columbia-0 Arabidopsis. For measurement of mutation rates, plants were grown in 100- × 2.5-mm petri dishes containing one-half-strength Murashige and Skoog salts, B5 vitamins, and 3% (w/v) Suc, solidified with 0.75% (w/v) agar. For selection of transformed plants, kanamycin was included at 25 mg L^{-1}. We compared mutation rates of plants grown on the same medium with 1% (w/v) Suc and found no significant difference; therefore 3% (w/v) Suc was used for all experiments. Seeds were surface-sterilized by treatment with 95% (v/v) ethanol for 1 h, and 50% (v/v) household bleach for 10 min, followed by four to five washes with sterile water. Sterilized seeds were evenly distributed in a grid pattern of 49 seeds per 100-mm petri dish, stratified at 4°C for 24 h, and placed in a growth chamber at 24°C under constant illumination with cool-white lamps at approximately 60 μmol m^{-2} s^{-1}. DNA was extracted with an efficiency of recovery of approximately 75% from six 2-week-old plants grown on 3% (w/v) Suc medium, using the method of Draper and Hays (2000). Plants grown under these conditions yielded an average of 1.4 μg DNA $plant^{-1}$, corresponding to an estimated 6.7×10^6 cells, similar to the estimates of Kovalchuk et al. (2000). Plants were grown for 14 d before scoring reversion of the GUS microsatellite transgene. For endogenous microsatellite assays, seeds from individual sole-grown plants were sterilized and plated on one-half-strength Murashige and Skoog media and grown for 10 to 12 d; whole plants were used for DNA preparations.

Construction of Microsatellite Reporter Genes and Transformation into Plants

The GUS microsatellite reversion reporters were derived from binary vector pBI221 (BD Biosciences Clontech, Palo Alto, CA). Restriction endonucleases *Bam*HI, *Eco*RI, *Sal*I, *Sma*I, *Asc*I, *Xba*I, and *Mfe*I were purchased from Invitrogen (Carlsbad CA). A 2,165-bp *Bam*HI-*Eco*RI fragment of pBI221 encoding GUS and a nopaline synthesis terminator was ligated into (*Bam*HI+*Eco*RI)-digested plasmid pBluescript SK+ (Stratagene) forming pGUS3. After removing the *Sal*I recognition site in the polylinker region of pGUS3, an in-frame *Sal*I restriction site was introduced immediately downstream of the initiating ATG codon of the *GUS* gene by PCR mutagenesis, as follows. A PCR product was templated by pBI221 DNA, using primer OGUS3 (5′-CCGATCCACCATGTCGACTTTACGTCCTGTAGAAACC-3′) encoding a *Bam*HI restriction site, a Kozak consensus translation signal upstream of the initiating ATG codon of *GUS*, and a *Sal*I restriction site immediately downstream, and primer OGUS1 (5′-CTTCCTGATTATTGACCCACAC-3′) 288 bp downstream of the *GUS* ATG. This product was the source of a *Bam*HI-*Mfe*I fragment used to replace the 5′ end of GUS in (*Bam*HI+*Mfe*I)-digested pGUS3, yielding pGUS5. Oligonucleotides with complementary regions were annealed to produce double-stranded DNA with ends complementary to *Sal*I-restricted pGUS5. To introduce an out-of-frame $(G)_7$ run, a double-stranded DNA fragment with staggered ends complementary to *Sal*I-restriction ends, made by annealing oligonucleotides G7SAL (5′-TCGAAGGGGGGGC-3′) with G7SAL (5′-TCGAGCCCCCCCT-3′), was ligated into *Sal*I-restricted pGUS5. $(G)_{10}$ and $(G)_{13}$ runs were introduced in an identical manner by annealing together oligonucleotides with internal G and C repeats. PCR analysis and DNA sequencing of the products confirmed orientation of the introduced nucleotides. Restriction of the sequence-confirmed intermediate plasmids with *Bam*HI and *Eco*RI released approximately 2.2-kb fragments—encoding the mutated GUS and terminator sequence—that were used to replace the wild-type GUS sequence in (*Bam*HI+*Eco*RI)-digested binary vector pBI221. Binary vectors were transformed into *Agrobacterium tumefaciens* strain EHA105 and maintained by kanamycin selection. Plants were transformed using the dipping method (Clough and Bent, 1998), and primary transformants were selected by plating 2,000 seeds $plate^{-1}$ onto media containing 50 mg L^{-1} kanamycin.

UV-C Irradiation of Plants

Nine-day-old plants grown in petri dishes were irradiated with 1,200 J m^{-2} of UV-C light produced by a bank of six 15-W Sylvania germicidal lamps at a distance of 125 cm. Dosage was calculated from measurements made with a Spectroline DRC-100X digital radiometer (Spectronics, Westbury, NY). Plants were immediately returned to growth chambers for 5 d and then histochemically stained, in parallel with unirradiated control plants to detect spots of GUS$^+$ (reverted) cells.

Histochemical Staining

Staining of 2-week-old plants was as described by Kovalchuk et al. (2000). In brief, plants were vacuum-infiltrated for 10 min with a solution of 333 mg L^{-1} 5-bromo-4-chloro-3-indolyl-β-D-glucuronide in 100 mM phosphate buffer, pH 7.0, and 0.1% (v/v) Triton X-100. After 48 h of incubation at 37°C, plants were decolorized in ethanol. Blue spots were counted manually under a stereo dissecting microscope. The exact tissue layers contributing to blue staining were not resolvable at this level of magnification.

Genotyping of Transgenic Plants

A modified cetyl-trimethyl-ammonium bromide method, as described by McClarvey and Kaper (1991), was used to prepare DNA from single leaves (for F_2 genotyping) or single cotyledons (for mutation rate analyses); DNA was resuspended in 10 or 30 μL of DNA buffer (10 mM Tris, pH 7.0 1mM EDTA), respectively. In PCR reactions templated with 1 μL of DNA, *AtMSH2*-specific primer OMSH30 (5′-CCAGTTGCCCTACTCCATACTG-3′) was paired with T-DNA-specific primer OLBA1 (5′-TGGTTCACG-TAGTGGGCCATC-3′), yielding a 544-bp fragment, or with *AtMSH2*-specific primer OMSH5 (5′-TTTCAGTGTCAATGTGAGCG-3′), yielding a 1,117-bp product. Typical PCR conditions were 94°C for 3 min followed by 30 cycles of 15 s at 94°C, 15 s at 54°C, and 1 min at 72°C. PCR products were separated by electrophoresis on 0.8% (w/v) agarose.

DNA Analyses

For DNA-blot (Southern) analysis of SALK_002708, 1 μg of *Eco*RV-digested wild-type or *AtMSH2*::T-DNA genomic DNA was electrophoresed

through 0.8% (w/v) agarose gels and transferred onto Magnacharge (Osmonics, Minnetonka, MN) nylon membrane. A 1.1-kb probe was PCR-amplified from Col-0 DNA using *AtMSH2*-specific primers OMSH21 (5′-GAGTGCTCTGTAGATCTTGACC-3′) and OMSH29 (5′-CAACTTG-AGCCATCAGCACAATC-3′) and then ^{32}P-radiolabeled using a DECAprime II kit (Ambion, Austin, TX). After overnight hybridization at 65°C, the blot was washed in 0.1% (w/v) SDS and 2× SSC for 30 min at room temperature followed by a final 65°C 1-h wash in 0.1% (w/v) SDS, 1× SSC. Southern-blot analysis of lines transformed with *GUS*-microsatellite alleles was identical except that 1 μg of DNA from each line that segregated 3:1 for kanamycin resistance was digested with *Eco*RI or *Bam*HI before electrophoresis and blotted as described above. Blots of DNA from GUS-microsatellite-transformed lines were probed with a ^{32}P-radiolabeled 534-bp *Hin*dIII fragment of *GUS* excised from pBI221 beginning 605 bp past the initiating *GUS* ATG codon.

Analysis of Microsatellite Instability

All microsatellite loci in this study (except T3F17, developed by us) were chosen from the list of nucleotide repeat sequences and respective primer pairs for PCR amplification of Bell and Ecker (1994). In some cases, new primers were designed, using Primer 3 software (http://www-genome.wi.mit.edu/cgi-bin/primer/primer3_www.cgi), to alter the length of the resultant PCR products so that a mixture of PCR products from all nine loci could be resolved by differential mobility and/or fluorescence in a single electrophoretic capillary tube. Oligonucleotides, one for each locus-pair labeled with hexachloro-6-carboxyfluorescein or 6-carboxyfluorescein fluorescent dyes, were obtained from MWG Biotech (Highpoint, NC). The following forward and reverse primers were used: ATEAT1, 5′-TGCGTGAATGATATG-TAACTGG-3′ and 5′-TTTGATTGCCTTATTTGTCTGC-3′; T3F17, 5′-CTGAGTTTATACCGTTGCATCC-3′ and 5′-AAAAAGTGGAAAAACCCT-ACCC-3′; NGA6, 5′-GACTAAAGTGGGTCCCTTGG-3′ and 5′-CACAC-CCAAAACTCGTAAAGC-3′; NGA8, 5′-TGGCTTTCGTTTATAAACATCC-3′ and 5′-GAGGGCAAATCTTTATTTCGG-3′; NGA139, 5′-GGTTTCGT-TTCACTATCCAGG-3′ and 5′-AGAGCTACCAGATCCGATGG-3′; NGA151, 5′-CCAGAGCTTGTTTTGGGAAG-3′ and 5′-TTTGATGAAACGGAATAT-AGAAAGC-3′; NGA168, 5′-GAGCTTGTGCCAGTGTCG-3′ and 5′-GGAGC-CTCGAATGATGAAGC-3′; NGA172, 5′-CATCCGAATGCCATTGTTC-3′ and 5′-AGCTGCTTCCTTATAGCGTCC-3′; and NGA1107, 5′-CGACGA-ATCGACACAATTACG-3′ and 5′-GGCTACAATAGTGGGAAAACG-3′. The reverse primers for loci ATEAT1, NGA151, NGA172, and NGA1107 were labeled with FAM fluorescent dye; the reverse primers for loci T3F17, NGA6, NGA8, NGA139, and NGA168 were labeled with HEX fluorescent dye. Initial denaturation at 94°C for 3 min was followed by 30 cycles of PCR amplification: 94°C for 30 s, 54°C for 30 s, and 72°C for 30 s, then a final 1-h incubation at 72°C. Up to nine locus-specific PCR reaction products were diluted as empirically found appropriate for subsequent analysis, mixed, and analyzed by capillary electrophoresis and measurement of DNA-bound fluorescent intensities, using the ABI Prism 3100 Genetic Analyzer and associated software (Applied Biosystems, Palo Alto, CA). Product sizes were precisely and reproducibly assigned by comparison with an internal lane standard using GeneScan software (GS400HD Rox, Applied Biosystems), although absolute size measurements differed from genome-predicted sizes. Electropherograms were generated using Genotyper software. Initially, DNA samples from 30 progeny of an *ATMSH2*$^{-/-}$ plant were amplified with radiolabeled primers for loci NGA6, NGA168, or T3F17, electrophoresed on a polyacrylamide gel and visualized by autoradiography, or were amplified with fluorescently labeled primers and analyzed with the ABI 3100 as described above. The two analytical methods identically detected shifts (or not) in the product band distributions generated by PCR slippage (see Fig. 2); all subsequent analyses employed the capillary-electrophoresis Genetic Analyzer technology. In all cases where product distributions appeared shifted, assays were repeated with an independent PCR amplification of DNA from the same plant.

Construction of dsRNA Vector

A dsRNA vector designed to silence *AtMSH2* was created as described on the Web site (http://www.chromdb.org/plasmids/pFGC5941.html) by inserting two identical fragments of *AtMSH2* in opposite orientations, flanking a 1.4-kb chalcone synthase intron under the control of a cauliflower mosaic virus 35S promoter into binary vector pFGC5941 (Arabidopsis Biological Resource Center, accession no. CD3–447). In brief, a 735-bp fragment of *AtMSH2* beginning at bp 829 of the coding sequence, was amplified from an *AtMSH2* cDNA clone (Culligan and Hays, 1997) using one primer designed to add *Swa*I and *Bam*HI recognition sites to the 5′ end of the PCR product paired with a downstream primer designed to add *Xba*I and *Asc*I sites to the 3′ end of the PCR product. A (*Swa*I+*Asc*I)-digested PCR product was ligated into the *Swa*I and *Asc*I sites of pFGC5941. An *Xba*I-*Bam*HI fragment of the original PCR product was subsequently ligated into the *Bam*HI and *Xba*I sites of the resultant intermediate plasmid. The final construct, pMSH2(RNAi), or empty vector pFGC9941 was transformed into *A. tumefaciens* strain EHA105 and used for parallel plant transformations.

ACKNOWLEDGMENTS

We thank Kevin Culligan for bringing to our attention the T-DNA mutant in the database. We thank the Salk Institute Genomic Analysis Laboratory for providing the sequence-indexed Arabidopsis T-DNA insertion mutants and the Arabidopsis Biological Resource Center Stock Center (Ohio State University, Columbus) for providing seeds.

Received March 21, 2003; returned for revision April 25, 2003; accepted May 31, 2003.

LITERATURE CITED

Ade J, Belzile F, Philippe H, Doutriaux M-P (1999) Four mismatch repair paralogues coexist in *Arabidopsis thaliana*: *AtMSH2*, AtMSH3, AtMSH6-1 and AtMSH6-2. Mol Gen Genet **262:** 239–249

Alani E, Sokolsky T, Studamire B, Miret JJ, Lahue RS (1997) Genetic and biochemical analysis of MSH2p-MSH6p: role of ATP hydrolysis and Msh2p subunit interactions in mismatch base pair recognition. Mol Cell Biol **17:** 2436–2447

Baker SM, Bronner CE, Zhang L, Plug AW, Robatzek M, Warren G, Elliott EA, Yu J, Ashley T, Arnheim N et al. (1995) Male mice defective in the DNA mismatch repair gene PMS2 exhibit abnormal chromosome synapsis in meiosis. Cell **82:** 309–319

Bell CJ, Ecker JR (1994) Assignment of 30 microsatellite loci to the linkage map of Arabidopsis. Genomics **19:** 137–144

Boyer JC, Yamada NA, Roques CN, Hatch SB, Riess K, Farber RA (2002) Sequence dependent instability of mononucleotide microsatellites in cultured mismatch repair proficient and deficient mammalian cells. Human Mol Genet **11:** 707–713

Chambers SR, Hunter N, Louis EJ, Borts RH (1996) The mismatch repair system reduces homeologous recombination and stimulates recombination-dependent chromosome loss. Mol Cell Biol **16:** 6110–6120

Chuang CF, Meyerowitz EM (2000) Specific and heritable genetic interference by double-stranded RNA in *Arabidopsis thaliana*. Proc Natl Acad Sci USA **97:** 4985–4990

Clough SJ, Bent AF (1998) Floral dip: a simplified method for *Agrobacterium*-mediated transformation of *Arabidopsis thaliana*. Plant J **16:** 735–743

Culligan KM, Hays JB (1997) DNA mismatch repair in plants: an *Arabidopsis thaliana* gene that predicts a protein belonging to the MSH2 subfamily of eukaryotic MutS homologs. Plant Physiol **115:** 833–839

Culligan KM, Hays JB (2000) Arabidopsis MutS homologs-AtMSH2, AtMSH3, AtMSH6, and a novel AtMSH7-form three distinct protein heterodimers with different specificities for mismatched DNA. Plant Cell **12:** 991–1002

Cupples CG, Cabrera M, Cruz C, Miller JH (1990) A set of *lacZ* mutations in *Escherichia coli* that allow rapid detection of specific frameshift mutations. Genetics **125:** 275–280

Degtyareva NP, Greenwell P, Hofmann ER, Hengartner MO, Zhang L, Culotti JG, Petes TD (2002) *Caenorhabditis elegans* DNA mismatch repair gene *msh-2* is required for microsatellite stability and maintenance of genome integrity. Proc Natl Acad Sci USA **99:** 2158–2163

Dong C, Whitford R, Langridge P (2002) A DNA mismatch repair gene links to the *Ph2* locus in wheat. Genome **45:** 116–124

Draper CK, Hays JB (2000) Replication of chloroplast, mitochondrial and nuclear DNA during growth of unirradiated and UVB-irradiated Arabidopsis leaves. Plant J 23: 255–265

Galbraith DW, Harkins KR, Knapp SJ (1991) Systemic endopolyploidy in *Arabidopsis thaliana*. Plant Physiol 96: 985–989

Gurtu VE, Verma S, Grossmann AH, Liskay RM, Skarnes WC, Baker SM (2002) Maternal effect for DNA mismatch repair in the mouse. Genetics 160: 271–277

Hays JB (2002) *Arabidopsis thaliana*, a versatile model system for study of eukaryotic genome-maintenance functions. DNA Repair 1: 579–600

Herwath M, Kramer W, Kunze R (2002) Structure and expression of the Zea *mays* mutS-homologs Mus1 and. Mus2 Theor Appl Genet 105: 423–430

Kolodner RD, Marsischky GT (1999) Eukaryotic DNA mismatch repair. Curr Opin Genet Dev 9: 89–96

Kovalchuk I, Kovalchuk O, Hohn B (2000) Genome-wide variation of the somatic mutation frequency in transgenic plants. EMBO J 19: 4431–4438

Kunkel TA, Bebenek K (2000) DNA replication fidelity. Annu Rev Biochem 69: 497–529

Loeb LA (1994) Microsatellite instability: marker of a mutator phenotype in cancer. Cancer Res 54: 5059–5063

Matic I, Rayssuguier C, Radmann M (1995) Interspecies gene exchange in bacteria: the role of SOS and mismatch repair systems in evolution of species. Cell 80: 507–515

McGarvey P, Kaper JM (1991) A simple and rapid method for screening transgenic plants using the PCR. Biotechniques 11: 428–432

Parsons R, Li G-M, Longley MJ, Fang W-H, Papadopoulus N, Jen J, de la Chapelle A, Kinzler KW, Vogelstein B, Modrich P (1993) Hypermutability and mismatch repair deficiency in RER+ tumor cells. Cell 75: 1227–1236

Reenan RA, Kolodner RD (1992) Characterization of insertion mutations in the *Saccharomyces cerevisiae* MSH1 and MSH2 genes: evidence for separate mitochondrial and nuclear functions. Genetics 132: 975–985

Reitmair AH, Schmits R, Ewel A, Bapat B, Redston M, Mitri A, Waterhouse P, Mittrucker HW, Wakeham A, Liu B et al (1995) MSH2 deficient mice are viable and susceptible to lymphoid tumours. Nat Genet 11: 64–70

Strand M, Prolla TA, Liskay RM, Petes TD (1993) Destabilization of tracts of repetitive DNA in yeast by mutations affecting DNA mismatch repair. Nature 365: 274–276

Tran HT, Keen JD, Kricker M, Resnick MA, Gordenin DA (1997) Hypermutability of homonucleotide runs in mismatch repair and DNA polymerase proofreading mutants. Mol Cell Biol 17: 2859–2865